Improving the accuracy of retrieved cardiac electrical conductivities

A. Kamalakkannan[1] P. R. Johnston[2] B. M. Johnston[3]

(Received 11 February 2022; revised 14 July 2022)

Abstract

Accurate values for the six cardiac conductivities of the bidomain model are crucial for meaningful electrophysiological simulations of cardiac tissue and are yet to be achieved. A two-stage optimisation process is used to retrieve the cardiac conductivities from cardiac potentials measured on a multi-electrode array—the first stage simultaneously fits all six conductivities, and the second stage fits a subset of the conductivities (intracellular conductivities), while holding the remainder of the conductivities (extracellular conductivities) constant. Previous studies have shown that the intracellular conductivities are retrieved to a lesser degree of accuracy than extracellular conductivities. This study tests the proposition that there exists a relationship between the extracellular and intracellular conductivities during the second stage of the optimisation that affects the accuracy of the retrieved intracellular

DOI:10.21914/anziamj.v63.17148, Published 2022-08-12, as part of the Proceedings of the 15th Biennial Engineering Mathematics and Applications Conference. ISSN 1445-8810. (Print two pages per sheet of paper.)

conductivities. A measure to quantify this relationship is developed using polynomial chaos. The results show that a significant relationship does exist, and thus any errors in the extracellular conductivities are magnified in the retrieved intracellular conductivities. Thus, it is suggested that future protocols for retrieving conductivities incorporate the uncertainty in the extracellular conductivities.

Contents

1 Introduction

Meaningful simulation studies of the heart are a helpful tool in facilitating an understanding of electrical conduction defects that cannot be achieved through experimental means alone [4]. The bidomain model [12] is commonly used to simulate cardiac potentials in two interpenetrating domains, extracellular $\mathbf{e}$ space and intracellular $\mathbf{i}$ space, through a continuum approximation. However, key parameters of the model, such as the cardiac conductivities, are yet to be determined with certainty.

Cardiac fibres are arranged in laminar sheets that are stacked with a slight offset from sheet to sheet to form the walls of the heart, thus leading to a rotation of fibres [10]. Current propagates in three directions—along and across the direction of the fibres (longitudinal $\mathfrak{l}$ and transverse $\mathfrak{t}$ directions, respectively), and normal to sheets of the fibres (normal $\mathfrak{n}$), thus requiring a total of six cardiac conductivity values: g_{il}, g_{it}, g_{in}, g_{el}, g_{et} and g_{en}.

Despite efforts over the past fifty years, difficulties associated with obtaining and interpreting experimental measurements have prevented researchers from obtaining accurate values for the cardiac conductivities. Several studies, working under various assumptions, were able to obtain a subset of the conductivities; however, a lack of consensus exists for the accepted retrieved values due to a large variance in results between the studies. Previous studies have proposed techniques to retrieve the cardiac conductivities through experimental or theoretical means, although no study has retrieved all six cardiac conductivities through experimental means alone [4].

The procedure for retrieving cardiac conductivities, considered here, first involves making cardiac potential measurements on a multi-electrode array, followed by a two-stage optimisation technique to estimate the cardiac conductivities. Johnston and Johnston [5] showed that a 75-electrode array was capable of retrieving all six cardiac conductivities using simulated data. However the intracellular conductivities (g_{il}, g_{it}, g_{in}) were retrieved less accurately than the extracellular conductivities (g_{el}, g_{et}, g_{en}).

Examining and understanding the difficulties faced in retrieving the intracellular conductivities can inform and aid in future efforts to determine these conductivities. Hence the primary focus of this study is to investigate the relationship between the extracellular and intracellular conductivities in the retrieval process using polynomial chaos techniques. Section 2 outlines the mathematical model, the measuring electrode array, the solution technique and the optimisation (inversion) process. Section 3 summarises the polynomial chaos techniques used in this study. The results of this study are presented in Section 4, followed by conclusions in Section 5.

2 Governing equations and inversion technique

To reduce the complexity of the solution techniques, the ventricular muscle is represented by a slab of cardiac tissue extending 2 cm in the x and y directions and 1 cm in the z direction and is assumed to be in contact with a pool of blood whose thickness extends to infinity. It is assumed that the longitudinal, transverse and normal directions are aligned along the x, y and z axes, respectively [8].

The distributions of the cardiac potentials through the intracellular and extracellular spaces are given by the bidomain governing equations [12]

$$\nabla \cdot M_i \nabla \phi_i = \frac{\beta}{R}(\phi_i - \phi_e), \quad \nabla \cdot M_e \nabla \phi_e = -\frac{\beta}{R}(\phi_i - \phi_e) - I_c, \qquad (1)$$

where ϕ_q is the potential ($q = i, e$), β is the ratio of surface cell area to cell volume, R is the specific resistance of the membrane separating the intracellular and extracellular domains and I_c is the current per unit volume applied in the extracellular space. Finally, M_q represents the conductivity tensor given by $M_q = RD_qR^T$ where D_q is a diagonal matrix that contains the conductivities in the longitudinal, transverse and normal directions for the respective space and R is a 3D rotation matrix about the z-axis [12].

Equation (1) is solved by first expanding ϕ_q as a Fourier series. Substituting the resulting expansions into the governing equations yields two sets of four ordinary differential equations which are then solved with a 1D finite difference scheme. A full description of the solution technique, the model, the boundary conditions, and the model assumptions is given by Johnston et al. [6].

The parameters used to solve the model are $\beta = 2000\,\mathrm{cm}^{-1}$, $R = 9100\,\Omega\,\mathrm{cm}^2$, $I_c = 1\ \mu\mathrm{A\,cm}^{-3}$, with the conductivity of the blood assumed to be 6.7 mS/cm and the rotation of the fibres assumed to be 120°. These parameters are consistent with values found in the literature [13, 9, 5]. The nominal conductivities used for the simulations are $g_{il} = 2.40$, $g_{it} = 0.24$, $g_{in} = 0.10$, $g_{el} = 2.40$, $g_{et} = 1.60$ and $g_{en} = 1.00$ in units of mS/cm [3].

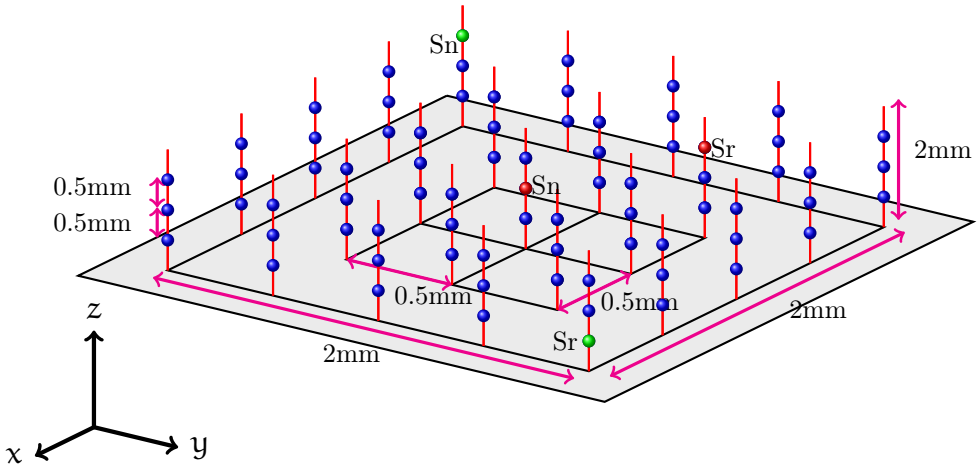

Figure 1: The 75-electrode multi-electrode array used for making the potential measurements [5]. Current source and sink electrodes are marked by Sr and Sn, respectively. Current electrodes used during the first and second-passes are marked red and green, respectively, and the measuring electrodes are marked blue. Electrodes are in layers named, from bottom to top, Layer 1, 2 and 3.

2.1 Electrode array and inversion

Cardiac potential measurements are made or simulated on a multi-electrode array that consists of 25 micro-needles, each containing three electrodes arranged in three planes (Figure 1), with the first layer of electrodes inserted 0.075 cm into the cardiac tissue. Two sets of measurements are made using this array, referred to as first-pass and second-pass measurements. For the first-pass measurements, the current source and sink electrodes are placed in a 'close' arrangement, during which the majority of the current propagates through the extracellular space. For the second-pass measurements, the current injection electrodes are widely-spaced and are placed diagonally on the array which results in a proportion of the current being re-directed into the intracellular space [5]. The specific configurations for the current source and sink electrodes for each measurement set are given in Figure 1.

Due to the non-linear dependence between the bidomain conductivities and the cardiac potentials, it is necessary to minimise the following Tikhonov functional [1] to obtain an approximation for the conductivities given in the vector $\mathbf{m}$:

$$\|\mathbf{G}(\mathbf{m}) - \boldsymbol{\phi}\|_2^2 + \gamma^2 \|\mathbf{m}\|_2^2, \tag{2}$$

where $\mathbf{G}$ is the forward model, $\boldsymbol{\phi}$ is the vector of measured potentials and γ is the regularisation parameter taken to be 10^{-2} [5]. The first-pass measurements are used to simultaneously fit g_{il}, g_{it}, g_{in}, g_{el}, g_{et} and g_{en}, that is $\mathbf{m} = [g_{il}, g_{it}, g_{in}, g_{el}, g_{et}, g_{en}]^T$ [5]. This is referred to as the first-pass inversion. Previous simulations have shown that a second-pass of this inversion process is required as the intracellular conductivities are not retrieved accurately in the first-pass inversion [9].

A second-pass inversion, using the second-pass measurement set, aims to refine the intracellular conductivities by fitting only these values, thus $\mathbf{m} = [g_{il}, g_{it}, g_{in}]^T$. The extracellular conductivities used in the second-pass inversion are held constant at their values found in the first-pass inversion. Although the second-pass aims to refine the accuracy of the intracellular conductivities, there is still a notable error in the retrieved values compared with the retrieved extracellular conductivities. As an example, two passes with 5% noise introduced to the nominal potentials retrieved the extracellular conductivities to a relative error of approximately 0.5%–1.5%, while the three intracellular conductivities had an average relative error of 6%–30% [5]. A more detailed explanation and recent advancements in the inversion process are given by Kamalakkannan et al. [7] and Sun et al. [11].

We hypothesise that holding the extracellular conductivities constant in the second-pass influences the accuracy of the retrieved intracellular conductivities. Referring to equation (2), errors in the extracellular conductivities during the second-pass produce potentials that deviate from the true values, thus affecting the retrieval of the intracellular conductivities. To verify this claim, a measure to quantify the influence of the extracellular conductivities on the second-pass cardiac potentials is required.

3 Generalised polynomial chaos

Generalised polynomial chaos (gPC) is utilised to approximate stochastic processes through an orthogonal polynomial expansion given that the distributions of the input parameters are known [14]. The resulting expansion can be exploited to estimate the propagation of uncertainty from the model inputs to the model outputs [15, 2].

A polynomial chaos expansion is constructed to approximate the cardiac potentials of the second-pass in terms of the six cardiac conductivities. We sample the cardiac conductivity from a uniform distribution within the range $[0.5M_0, 1.5M_0]$ where M_0 is the nominal value of the conductivity. Legendre orthogonal polynomials up to the sixth order are used to construct the expansion [15]. The resulting expansion accurately approximates the cardiac potentials to an L_2 relative error norm of the order 2×10^{-4}. We find changing the polynomial order to seven gave an L_2 relative error norm of approximately 8×10^{-5}, while lower polynomial orders produced a relatively inaccurate expansion (L_2 relative error norm of approximately 3×10^{-3} for polynomial order five).

Recall that we are trying to quantify the influence of the extracellular conductivities during the second-pass. That is, we are interested in determining the contribution of the extracellular conductivities to the total variance of the cardiac potentials. The total variance of the cardiac potentials is approximated by taking the variance of the polynomial expansion. Rather than determining all the contributions to the total variance due to the extracellular conductivities, it is more efficient to determine the contributions to the total variance due to the interactions between the intracellular conductivities and then taking the complement of this value. That is,

$$Q_e = 1 - \frac{\sum_{\alpha \in \mathbb{A}_i} \mathbb{V}[c_\alpha \Psi_\alpha]}{\mathbb{V}[Y]}, \tag{3}$$

where Y is a vector of cardiac potentials, c_α are the expansion coefficients, Ψ_α are the Legendre polynomials, $\alpha = \{\alpha_1, \alpha_2, \ldots, \alpha_6\}$ are the set of multi-

indices, $\mathbb{A}_i$ is the set of multi-indices $\boldsymbol{\alpha}$ that contains the parameters associated with the intracellular conductivities, and $\mathbb{V}$ is the variance operator. The closer Q_e is to 1, the greater the influence of the extracellular conductivities on the cardiac potentials during the second-pass. A detailed explanation of gPC, estimating the expansion coefficient and the variances, is given by Xiu and Karniadakis [15].

4 Results and discussion

4.1 Influence of extracellular conductivities during the second-pass

Figure 2 presents the Q_e value for each measuring electrode during the second-pass. The results are presented on the three planes of the electrode array that contain the electrodes in Layer 1, Layer 2 and Layer 3 (Figure 1).

Figure 2 shows that Q_e is fairly close to one throughout the array with $Q_e > 0.82$ at all measuring electrodes. This indicates that the extracellular conductivities have a significant influence during the second-pass. This influence tends to be approximately symmetric along the line of the current injection electrodes. The quantity Q_e also tends to be greater along the horizontal boundaries of the array, while the measure is at a minimum in the middle of the electrode array on Layer 2. We believe Q_e is at its lowest value due to the symmetry of the current electrodes.

The results suggest that small errors in the extracellular conductivities during the second-pass considerably affect the calculated potentials ($\mathbf{G}$ from equation (2)), moving them away from the actual potential distribution. Consequently, this affects the retrieval of the intracellular conductivities.

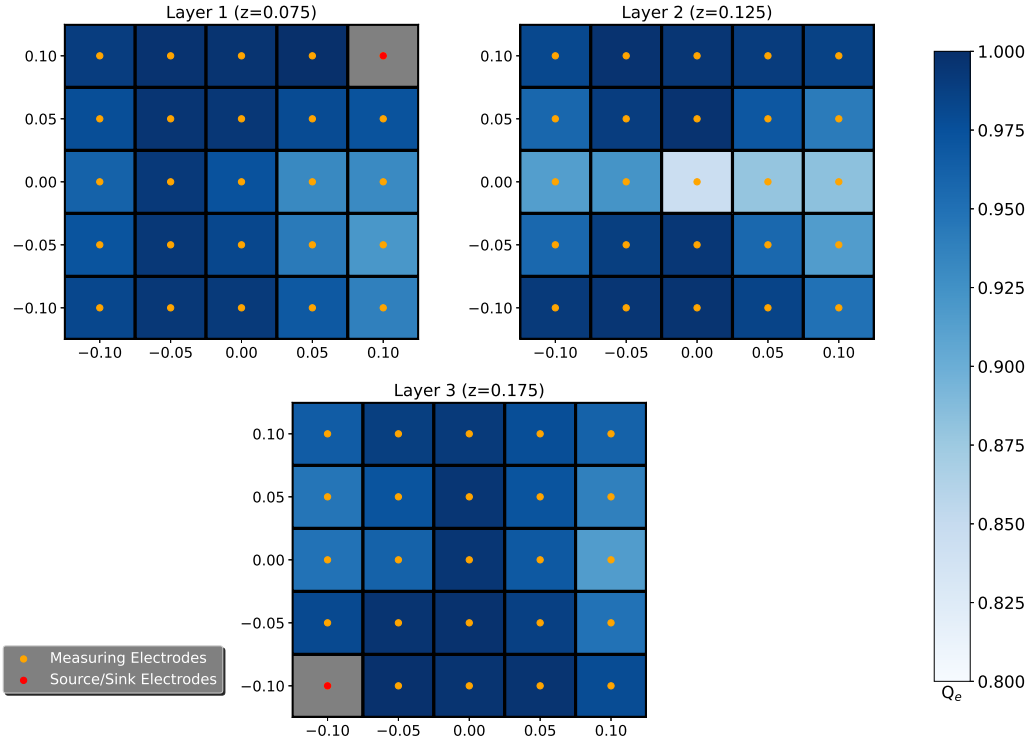

Figure 2: The Q_e values at the measuring electrodes during the second-pass. Red nodes, and the grey segments, represent the positions of the current electrodes, while the yellow nodes represent the measuring electrodes.

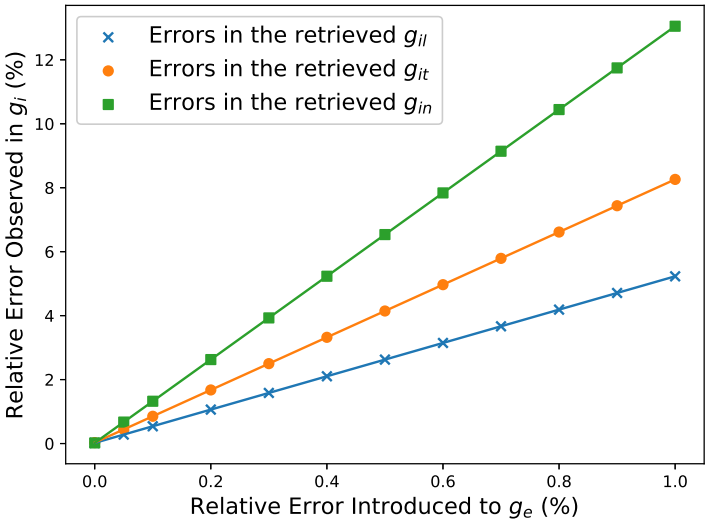

Figure 3: Relative errors of the retrieved intracellular conductivities for a range of errors introduced to the extracellular conductivities.

4.2 Verifying the influence of the extracellular conductivities during the second-pass

The influence of the extracellular conductivities during the second-pass is now verified by simulating a second-pass inversion with a small constant error introduced to all three extracellular conductivities. By not introducing experimental noise to the second-pass measurements, we ensure that any errors in the retrieved intracellular conductivities are exclusively a consequence of the errors introduced to the extracellular conductivities. Note that the study presented here is not reflective of the actual inversion process but only aims to provide a rudimentary illustration of the influence of the extracellular conductivities during the second-pass. Figure 3 presents the results of this study.

Analysing Figure 3, it is evident that errors in the extracellular conductivities

during the second-pass are magnified in the retrieved intracellular conductivities. A linear relationship is present between the errors of the extracellular and intracellular conductivities; however, this is due to the simplification of the problem where the same error is introduced to all three extracellular conductivities. The results suggest that g_{in} is most influenced by errors in the extracellular conductivities, followed by g_{it} and g_{il}.

5 Conclusion and future recommendations

This article examined some of the difficulties associated with obtaining accurate intracellular cardiac conductivity values. It was hypothesised that the extracellular conductivities used in the second-pass govern the accuracy of the retrieved intracellular conductivities. Thus a measure to quantify the influence of the extracellular conductivities during the second-pass was developed. Results indicate that obtaining accurate extracellular conductivities is crucial, as minor errors in these values can adversely affect the retrieval of the intracellular conductivities during the second-pass. Thus a protocol that incorporates the uncertainty of the extracellular conductivities during the second-pass might aid in the retrieval of the intracellular conductivities. Current research is investigating the possible use of Bayesian inference techniques for conductivity estimation, as such techniques are able to evaluate the uncertainty in the conductivity parameters and incorporate this uncertainty into later inferences.

Acknowledgments We acknowledge funding from the National Institutes of Health, Bethesda, USA (R03EB029625).

References

[1] R. C. Aster, B. Borchers, and C. H. Thurber. *Parameter Estimation and Inverse Problems*. Elsevier, 2018. DOI: 10.1016/C2015-0-02458-3 (cit. on p. C159).

[2] W. Huberts, W. P. Donders, T. Delhaas, and F. N. van de Vosse. "Applicability of the polynomial chaos expansion method for personalization of a cardiovascular pulse wave propagation model". In: *Int. J. Numer. Meth. Biomed. Eng.* 30.12 (2014), pp. 1679–1704. DOI: 10.1002/cnm.2695 (cit. on p. C160).

[3] B. M. Johnston, S. Coveney, E. T. Y. Chang, P. R. Johnston, and R. H. Clayton. "Quantifying the effect of uncertainty in input parameters in a simplified bidomain model of partial thickness ischaemia". In: *Med. Bio. Eng. Comput.* 56.5 (2018), pp. 761–780. DOI: 10.1007/s11517-017-1714-y (cit. on p. C157).

[4] B. M. Johnston and P. R. Johnston. "Approaches for determining cardiac bidomain conductivity values: Progress and challenges". In: *Med. Bio. Eng. Comput.* 58 (2020), pp. 2919–2935. DOI: 10.1007/s11517-020-02272-z (cit. on pp. C155, C156).

[5] B. M. Johnston and P. R. Johnston. "Determining six cardiac conductivities from realistically large datasets". In: *Math. Biosci.* 266 (2015), pp. 15–22. DOI: 10.1016/j.mbs.2015.05.008 (cit. on pp. C156, C157, C158, C159).

[6] B. M. Johnston, P. R. Johnston, and D. Kilpatrick. "A new approach to the determination of cardiac potential distributions: Application to the analysis of electrode configurations". In: *Math. Biosci.* 202.2 (2006), pp. 288–309. DOI: 10.1016/j.mbs.2006.04.004 (cit. on p. C157).

[7] A. Kamalakkannan, P. R Johnston, and B. M. Johnston. "A modified approach to determine the six cardiac bidomain conductivities". In: *Comput. Bio. Med.* 135, 104549 (2021). DOI: 10.1016/j.compbiomed.2021.104549 (cit. on p. C159).

[8] I. J. Legrice, P. J. Hunter, and B. H. Smaill. "Laminar structure of the heart: A mathematical model". In: *Am. J. Physiol. Heart Circ. Physiol.* 272.5 (1997), H2466–H2476. DOI: 10.1152/ajpheart.1997.272.5.H2466 (cit. on p. C157).

[9] R. Plonsey and R. Barr. "The four-electrode resistivity technique as applied to cardiac muscle". In: *IEEE Trans. Bio-med. Eng.* 29.7 (1982), pp. 541–546. DOI: 10.1109/tbme.1982.324927 (cit. on pp. C157, C159).

[10] D. D. Streeter Jr, H. M. Spotnitz, D. P. Patel, J. Ross Jr, and E. H. Sonnenblick. "Fiber orientation in the canine left ventricle during diastole and systole". In: *Circ. Res.* 24.3 (1969), pp. 339–347. DOI: 10.1161/01.res.24.3.339 (cit. on p. C156).

[11] M. Sun, N. M. S. de Groot, and R. C. Hendriks. "Cardiac tissue conductivity estimation using confirmatory factor analysis". In: *Comput. Bio. Med.* 135, 104604 (2021). DOI: 10.1016/j.compbiomed.2021.104604 (cit. on p. C159).

[12] L. Tung. "A Bi-Domain Model for Describing Ischemic Myocardial D-C Potentials." Thesis. Massachusetts Institute of Technology, 1978. URL: http://hdl.handle.net/1721.1/16177 (cit. on pp. C155, C157).

[13] S. Weidmann. "Electrical constants of trabecular muscle from mammalian heart". In: *J. Physiol.* 210.4 (1970), pp. 1041–1054. DOI: 10.1113/jphysiol.1970.sp009256 (cit. on p. C157).

[14] N. Wiener. "The homogeneous chaos". In: *Am. J. Math.* 60.4 (1938), pp. 897–936. DOI: 10.2307/2371268 (cit. on p. C160).

[15] D. Xiu and G. E. Karniadakis. "The Wiener–Askey polynomial chaos for stochastic differential equations". In: *SIAM J. Sci. Comput.* 24.2 (2002), pp. 619–644. DOI: 10.1137/S1064827501387826 (cit. on pp. C160, C161).

Author addresses

1. **A. Kamalakkannan**, School of Environment and Science, Griffith University, Nathan, QLD 4111, Australia.
mailto:a.kamalakkannan@griffith.edu.au
orcid:0000-0003-1987-4122

2. **P. R. Johnston**, School of Environment and Science, Griffith University, Nathan, QLD 4111, Australia.
orcid:0000-0002-8643-3901

3. **B. M. Johnston**, School of Environment and Science, Griffith University, Nathan, QLD 4111, Australia.
orcid:0000-0001-5889-8501